COMPUTATIONAL PLASTICITY

Fundamentals and Applications

Proceedings of the Fifth International Conference on
Computational Plasticity
held in Barcelona, Spain
17th-20th March 1997

PART 1

Edited by

D.R.J. Owen
Department of Civil Engineering , University of Wales
Swansea, U.K.

E. Oñate
Universidad Politécnica de Cataluña
Barcelona, Spain

E. Hinton
Department of Civil Engineering, University College
Swansea, U.K.

A publication of **CIMNE**

International Center for Numerical Methods
in Engineering (CIMNE)
Barcelona, Spain

YEARS
CIMNE
1987-1997

COMPUTATIONAL PLASTICITY
Fundamentals and Applications
D.R.J. Owen, E. Oñate and E. Hinton (Eds.)

NUMERICAL SIMULATION OF TEXTURE DEVELOPMENT OF POLYCRYSTALS UNDERGOING LARGE PLASTIC DEFORMATIONS

A. Bertram, T. Böhlke
Otto-von-Guericke-Univ. Magdeburg
Institut für Mechanik
Universitätsplatz 2
D-39106 Magdeburg
GERMANY

M. Kraska
Technische Universität Berlin
Institut für Mechanik
Sekr, C8, Str. d. 17 Juni 135
D-10623 Berlin
GERMANY

Abstract. The dependence of the macro stress on the macro deformation of the polycrystalline aggregate is simulated by using a representative volume element.

The texture development and its influence on the elastic response and on yield loci, defined by different criteria, are discussed.

1 INTRODUCTION

Large inelastic deformations of polycrystalline materials may occur during metal forming processes such as rolling, forging, drawing, or extrusion. Such processes are accompanied by considerable change in the macroscopic material behaviour due to microstructural changes.

Within certain limitations, crystal plasticity can be described using the concept of slip systems. This concept is capable of accounting for lattice rotations at large strains and uses a one-dimensional material law.

On the grain level, the material is heterogeneous due to the different orientations. To obtain the average macroscopic response of the aggregate, the so–called *homogenization* problem has to be solved.

In the present work, the *Representative Volume Element* (RVE) concept is used. At some macroscopic material point, a small volume is cut out of the body. For this volume, a boundary value problem is solved. This approach is principally capable of accounting for equilibrium and compatibility everywhere in the microscopically heterogeneous structure.

Based on the RVE–concept, the following numerical examples are presented: texture evolution and yield loci for different yield criteria in simple shear of an aluminium sample, and induced anisotropy of the elastic behaviour after uniaxial extension.

2 REPRESENTATIVE VOLUME ELEMENT

Homogenization procedure. Our aim is to obtain a relation at some material point P of the body between the local stress field $\mathbf{T}(P)$ and the global stress $\bar{\mathbf{T}}$, as well as between the local deformation field $\mathbf{F}(P)$ and the global deformation $\bar{\mathbf{F}}$. The basic idea is to split the displacement field $\mathbf{u}(P)$ into two parts, one corresponding to the homogeneous global deformation, and the other to a local fluctuating part $\mathbf{w}(P)$

$$\mathbf{u}(P) = (\bar{\mathbf{F}} - \mathbf{I})\mathbf{X}(P) + \mathbf{w}(P), \qquad (1)$$

where $\mathbf{X}(P)$ is the initial position vector of P and $\mathbf{I}$ is the unit tensor. The Taylor model is contained in the present one by setting $\mathbf{w}(P) = 0$, $\forall P \in \mathcal{B}$. Assuming the displacement fluctuation $\mathbf{w}$ to vanish or to be periodic on the boundary of the RVE, the global deformation gradient $\bar{\mathbf{F}}$ can be shown to be equal to the mean value of the local deformation gradient $\mathbf{F}$, where the corresponding average is taken over the volume in the initial placement

*Otto-v.-Guericke-Universität Magdeburg, Institut für Mechanik, Universitätsplatz 2, D-39106 Magdeburg

†Technische Universität Berlin, Institut für Mechanik, Sekr. C8, Str. d. 17. Juni 135, D-10623 Berlin

κ_0 (see [6], p.363)

$$\bar{\mathbf{F}} = \frac{1}{V_0}\int_{\kappa_0(\mathcal{B})} \mathbf{F}(P)\mathrm{d}V_0. \qquad (2)$$

A similar expression can be found for the Cauchy stress. Here the integral has to be taken over the volume in the actual placement κ

$$\bar{\mathbf{T}} = \frac{1}{V}\int_{\kappa(\mathcal{B})} \mathbf{T}(\kappa)\mathrm{d}V. \qquad (3)$$

Boundary conditions. In order to obtain the overall stress response $\bar{\mathbf{T}}$, displacement boundary conditions have to be imposed. The authors favour periodic boundary conditions because they avoid the stiffening effect of the homogeneous boundary conditions, where the displacements are set to the global ones.

Here, however, the displacement fluctuation field is forced to be periodic by setting it equal at corresponding points of opposite boundaries. Using the displacement split formulation, this can be done independently of the conditions for the overall average deformation.

Spatial discretization. For the calculation of the stress response to a given deformation process, we use a three-dimensional nonlinear finite-element approach. The RVE is discretized by tetrahedral elements. The minimal number of elements is determined by the required grain number and deformation resolution inside the grains.

The nodal displacement vectors $\mathbf{u}_K$ are decomposed according to the global placement split:

$$\mathbf{u}_K = (\bar{\mathbf{F}} - \mathbf{I})\mathbf{X}_K + \mathbf{w}_K \qquad (4)$$

with $\mathbf{X}_K$ the initial position of node K, and $\mathbf{w}_K$ the actual nodal fluctuation. Using this decomposition, the application of homogeneous or periodic boundary conditions follows simply by a reduction of the global system [5].

In the numerical simulations, an RVE with $7\times7\times7$ nodes is used. The structure contains 1080 tetrahedral elements and 645 degrees of freedom. Combining five tetrahedral elements in one grain, there are initially 216 independent orientations in the RVE. Due to the inhomogeneity of the deformation process, the orientations within the grains become inhomogeneous, too.

Initial grain orientations. As a first example, the initial state for our simulations was chosen to be isotropic. Such isotropy can be expected for polycrystals consisting of a large number of randomly oriented grains. However, the isotropy is very poor for small numbers of grains [7]. A considerable improvement can be obtained by an optimization starting from random orientation sets. Experience shows that RVEs produced in such a way behave sufficiently isotropic even for a rather small number of grains. The set used in the present work is shown in Fig. 1.

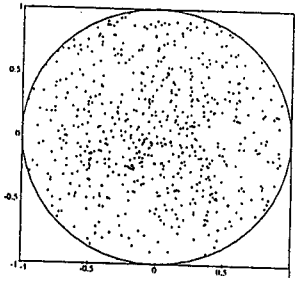

Figure 1. Initial (100) poles of the 216 grains

3 THE CONSTITUTIVE MODEL

Each grain is assumed to be a single crystal. The stresses are determined by the elastic deformations of the lattice, whereas the inelastic deformations relate material vectors to current lattice vectors. The model is based on the assumption of elastic ranges, in which the stresses are determined by a linear, anisotropic law

$$\mathbf{S} = \mathbb{K}_t[\mathbf{C} - \mathbf{C}_{Ut}]. \qquad (5)$$

$\mathbf{S} := \mathbf{F}^{-1}\mathbf{T}\mathbf{F}^{-\mathrm{T}}$ being a material stress tensor, $\mathbf{C}$ the right Cauchy Green tensor, $\mathbf{C}_{Ut}$ that one of an unloaded placement,

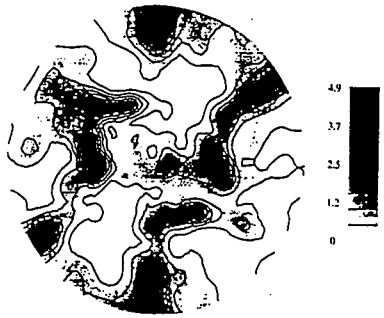

Figure 2. Shear texture, (100)–poles.

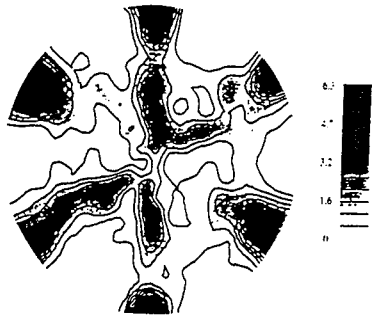

Figure 3. Shear texture, (111)–poles.

and $\mathbb{K}_t$ the forth order elasticity tensor. The index t indicates the time dependence of this law, which is related to the current elastic range. This dependence can be removed by the second assumption, which states, that the elastic laws of all possible elastic ranges are isomorphic. As a result, the current elastic law can be transformed into a time–independent reference law by the isomorphy condition

$$\mathbb{K}_t[\mathbf{C} - \mathbf{C}_{Ut}] = \mathbf{P}\mathbb{K}_0[\mathbf{P}^{\mathrm{T}}\mathbf{C}\mathbf{P} - \mathbf{C}_{U0}]\mathbf{P}^{\mathrm{T}}, \qquad (6)$$

where $\mathbf{P}$ is an invertible second order tensor, called plastic transformation [3, 4].

The linear elastic behaviour of fcc single crystals is described by three constants. In the numerical examples the slip system theory with octahedral slip systems is applied. As long as the resolved shear stresses $\tau_\alpha = \mathrm{tr}(\mathbf{S}\,\mathbf{d}_\alpha\otimes\mathbf{n}^\alpha)$ of all slip systems $(\mathbf{d}_\alpha, \mathbf{n}^\alpha)$ are below the critical ones $\tau_{c\alpha}$, no slip occurs according to Schmid's law and $\mathbf{P}$ remains constant. If, however, $|\,\tau_\alpha\,| \geq \tau_{c\alpha}$, the slip system can be activated and the rate of $\mathbf{P}$ is given by

$$\dot{\mathbf{P}}\mathbf{P}^{-1} = \sum_\alpha -\dot{\mu}_\alpha \mathbf{d}_\alpha \otimes \mathbf{n}^\alpha \qquad (7)$$

where the sum is taken over all active slip systems. $\dot{\mu}_\alpha$ is the slip rate in the particular slip system. This rate is related to the resolved shear stress by a Bingham–type constitutive relation

$$\dot{\mu}_\alpha = 1/\eta\,\mathrm{sign}(\tau_\alpha)\,|\,\tau_\alpha - \tau_{c\alpha}\,|\,. \qquad (8)$$

As a result, the material is elasto–viscoplastic.

The hardening is assumed to be isotropic on the slip system level. The critical shear stresses are initially equal in all slip systems and can be affected by slip in their slip system and in the other ones. The ratio of latent to self hardening is taken to be 1.4. The evolution equation for the critical shear stresses is given by

$$\dot{\tau}_{c\alpha} = h_0 \sum_\beta h_{\alpha\beta}\frac{\tau_{\mathrm{sat}} - \tau_{c\beta}}{\tau_{\mathrm{sat}} - \tau_{c0}}\dot{\mu}_\beta, \qquad (9)$$

$$h_{\alpha\beta} = \begin{cases} 1 & \text{if } \alpha = \beta, \\ 1.4 & \text{if } \alpha \neq \beta \end{cases} \qquad (10)$$

4 NUMERICAL EXAMPLE I

Williams [9] determines the texture, produced by simple shear in a polycrystalline sample of aluminium. The sample is sheared up to a shear magnitude k of 2.2. He obtains (111) and (100) pole projections in the plane containing the shear direction and the shear plane normal.

For the numerical simulation the following parameters have been used: $E = 63\,GPa$ (Young's modulus), $G = 28\,GPa$ (shear modulus), $\nu = 0.36$ (Poisson's ratio) [8]. The constants $\tau_{c0} = 0.1\,GPa$, $h_0 = 0.08\,GPa$ und $\tau_{\mathrm{sat}} = 0.164\,GPa$ have been chosen so that the relation (9) fits a slip system hardening relationship given by Becker [1].

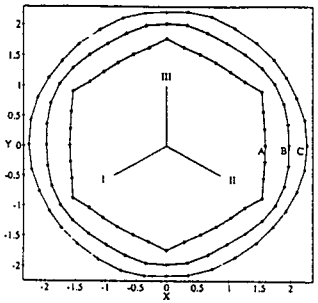

Figure 4. Initial yield loci (power criterion, $A = 3\%, B = 50\%, C = 99\%$.)

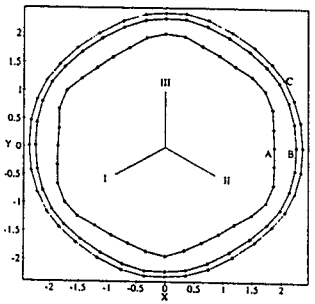

Figure 5. Initial yield loci (strain criterion, $A = 0.01\%, B = 0.1\%, C = 0.2\%$.)

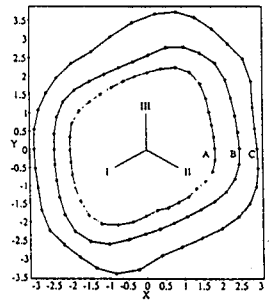

Figure 6. Yield loci at $k = 2.2$, (power crit. $A = 40\%, B = 70\%, C = 95\%$.)

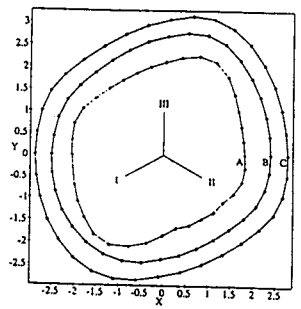

Figure 7. Yield loci at $k = 2.2$, (strain crit. $A = 0.01\%, B = 0.1\%, C = 0.2\%$.)

Starting from the isotropic and stress-free state, a constant deformation rate is imposed on the RVE until the global shear number reaches the value $k = 2.2$. The strain rate is chosen such that the global stress–strain curve is almost independent of the viscosity used in the flow rule on the slip system level.

Texture. Using linear density distributions assigned to the element orientations, density plots have been constructed (Fig. 2,3). In these plots the horizontal axis corresponds to the shear direction, the vertical one to the shear plane normal. The simulations start from a nearly isotropic state, whereas the experiments in [9] were done with cold rolled sheet material with a corresponding texture. Nevertheless, the location and value of highest density values in the (111) pole figures are in good agreement. However, in the (100) pole figure, two experimental maxima are missing.

Global yield loci. To determine the initial yield surface, isochoric deformation processes have been performed such that the stress paths in the deviatoric plane are equidistant. On these stress paths, different yield criteria are evaluated. In experiments, the yielding of a specimen can be indicated by different measures, such as the residual deformation after an elastic unloading process, or the decrease of the stiffness from the pure elastic value.

The RVE model offers the facility to use the physically relevant information about the slip system activity. The ratio $p := p_{\text{diss}}/p_{\text{tot}}$ of the mean dissipation rate

$$p_{\text{diss}} = \frac{1}{V_t} \int_{V_t} \sum_{i=1}^{12} \tau_i \dot{\mu}_i \mathrm{d}V \qquad (11)$$

to the total stress power $p_{\text{tot}} := \text{tr}(\tilde{\mathbf{T}}\tilde{\mathbf{D}})$ defines a normalized average indicator for yielding. As the global stress-strain–curve is nearly rate independent, the residual strain after an elastic unloading can be estimated by the present stress and the known elastic law. A one–dimensional measure d can be defined as the Frobenius norm of the residual strain. Figures 4 and 5 show the initial loci for different values of p and d The projection of the axes of the main stresses in this space are symmetry lines of the yield loci, thus indicating isotropy of the elastic–plastic transition behaviour. Furthermore, it turns out that fine criteria ($p \approx 3\%, d \approx 0.01\%$) are of Tresca type, coarse ones ($p \approx 50\%, d \approx 0.1\%$) tend to the v. Mises type. Figures 6 and 7 show the yield loci of the sheared RVE. For a globally unloaded state with residual stresses, the power criterion does not start at $p = 0$ when loaded again. No symmetry line is observed. The transition behaviour is anisotropic due to texture development and accumulated residual stresses.

5 NUMERICAL EXAMPLE II

The second example is a simulated uniaxial isochoric tensile test up to 300% elongation. The elastic parameters of the fcc grains are set to $E = 124\,GPa$, $G = 133\,GPa$, $\nu = 0.279$, as found for SRR 99, a Ni based super-alloy. The slip system parameters are assumed to be $\tau_{c0} = 1\,GPa$, which does not correspond to a particular material. Hardening effects are not considered here, thus $h_0 = 0$ in (9).

Texture. As to be expected, the texture consists of a (100) and a (111) fibre in tensile direction. The Rodrigues space representation, as used, e.g., by [1, 2], is given in Fig. 8,9, where the x-axis corresponds to the tensile axis. Choosing a fixed reference orientation, any orientation is represented by a spatial rotation. This rotation has an axis n and an angle φ between 0 and 180°. As such, the Rodrigues vector is a vector r of direction n and length $|\,\mathbf{r}\,| = \tan(\varphi/2)$.

In the inverse pole figure, reduction using fcc crystal symmetries leads to the orientation triangle. A similar reduction can be performed in Rodrigues space. The fundamental region has the shape of a cube centered at 0 with the corners cut off. The (100) fibre appears as a scattered band along the tensile axis (x), whereas the four skew bands near the edges of the fundamental region represent the (111) component.

Global elastic behaviour. The resulting stiffness tensors of the global elastic behaviour are determined before and after the deformation. In the initial state, the elastic behaviour is nearly isotropic. The corresponding Lamé constants are $\lambda = 220\,GPa$ and $\mu = 96.5\,GPa$. After the deformation, the elastic behaviour is transversely isotropic, due to evolution of a fibre texture in tensile direction (Fig. 10). However, the effect is rather limited, and thus may be negligible for many engineering purposes.

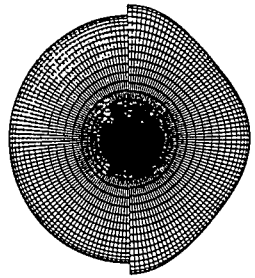

Figure 10. Young's modulus before (left) and after (right) extension (tensile axis horizontal in plane)

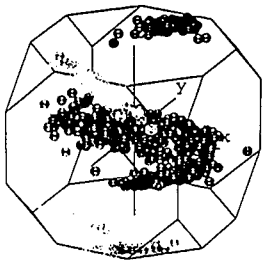

Figure 8. Grain orientations projected to the fundamental region.

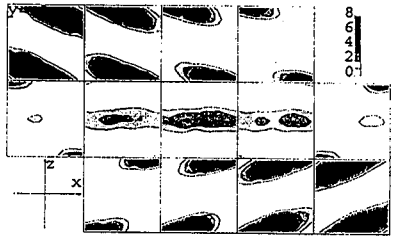

Figure 9. Orientation density in equidistant sections normal to the tensile axis.

6 CONCLUSIONS

Using a model for the description of finite inelastic deformations of single crystals, as well as the concept of a representative volume element, simulations of shear tests on polycrystalline specimens as reported in [9] have been carried out. Due to lack of data, assumptions concerning the initial texture had to be made.

The initial and subsequent yield loci have been examined using different yield indicators. In the initial state, fine criteria are of Tresca type and coarse ones are of v. Mises type, thus indicating isotropy of the elastic-plastic transition behaviour. As to be expected, this isotropy is completely lost after extreme plastic deformation.

The influence of the texture on the elastic behaviour has been demonstrated in a tensile test simulation.

REFERENCES

[1] R. Becker. Analysis of texture evolution in channel die compression – I. Effects of grain interaction. *Acta metall. mater.*, 39(6):1211–1230, 1991.

[2] R. C. Becker and S. Panchanadeeswaran. Crystal rotations represented as rodrigues vectors. *Textures Microstruct.*, 10:167–194, 1989.

[3] A. Bertram and M. Kraska. Description of finite plastic deformations in single crystals by material isomorphisms. In D. F. Parker and A. H. England, editors, *IUTAM Symposium on Anisotropy, Inhomogeneity and Nonlinearity in Solid Mechanics*, pages 77–90, Nottingham, UK, 1994. Kluwer Academic Publishers.

[4] A. Bertram and M. Kraska. Determination of finite plastic deformations in single crystals. *Arch. Mech.*, 47(2):203–222, 1995.

[5] M. Kraska and A. Bertram. Simulation of polycrystals using an FEM-based representative volume element. *Technische Mechanik*, 16:51–62, 1996.

[6] A. Krawietz. *Materialtheorie.* Springer, 1986.

[7] H. Takahashi et al. Elastic-plastic finite element polycrystal model. *International Journal of Plasticity*, 10(1):63–80, 1994.

[8] Ch. Weißmantel, C. Hamann, et al. *Grundlagen der Festkörperphysik.* Deutscher Verlag der Wissenschaften, Berlin, 1979.

[9] O. W. Williams. Shear textures in copper, brass, aluminum, iron and zirconium. *Trans. Met. Soc. AIME*, 224:129–139, 1962.